

# Effects of the Physicochemical Properties of Rutile Titania Powder on Photocatalytic Water Oxidation

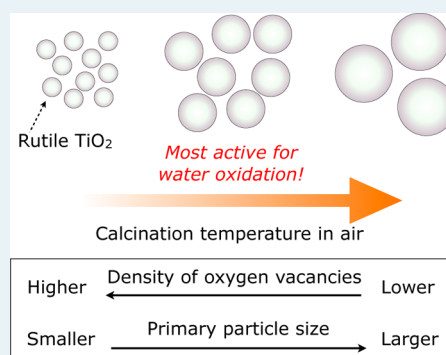
Kazuhiko Maeda<sup>\*,†,‡</sup>

<sup>†</sup>Department of Chemistry, Graduate School of Science and Engineering, Tokyo Institute of Technology, 2-12-1 NE-2 Ookayama, Meguro-ku, Tokyo 152-8550, Japan

<sup>‡</sup>Precursory Research for Embryonic Science and Technology (PRESTO), Japan Science and Technology Agency (JST), 4-1-8 Honcho, Kawaguchi, Saitama 332-0012, Japan

## Supporting Information

**ABSTRACT:** Water oxidation to form molecular O<sub>2</sub> over illuminated rutile TiO<sub>2</sub> powder in the presence of a reversible electron acceptor (IO<sub>3</sub><sup>−</sup> or Fe<sup>3+</sup>) was studied with respect to the effects of the physicochemical properties of rutile TiO<sub>2</sub>. Commercially available nanoparticulate rutile was calcined in air at 873–1273 K for 2 h to prepare crystallized rutile with varying particle sizes. Calcination at 1073 K resulted in the highest activity, regardless of the electron acceptor employed. High-temperature calcination facilitated crystallization of the rutile particles, enhancing the activity, while also reducing the oxygen vacancy density, thus lowering the material's charge transport capability.



**KEYWORDS:** heterogeneous photocatalysis, rutile, solar energy conversion, titania, water splitting

Since Fujishima and Honda demonstrated photoelectrochemical water splitting into H<sub>2</sub> and O<sub>2</sub> using a single-crystal rutile TiO<sub>2</sub> anode and a Pt cathode under ultraviolet (UV) irradiation in the presence of a chemical bias,<sup>1</sup> photocatalytic reactions on illuminated semiconductor particles have been extensively studied for the purpose of light-to-chemical energy conversion.<sup>2</sup> TiO<sub>2</sub> is one of the most widely studied semiconductor photocatalysts,<sup>3</sup> and anatase and rutile are both representative crystal structures of TiO<sub>2</sub>. Although anatase TiO<sub>2</sub> has been studied in various photocatalytic applications, only minimal research has been performed regarding the properties of rutile TiO<sub>2</sub> as a photocatalyst. Nevertheless, rutile TiO<sub>2</sub> possesses unique photocatalytic properties. For example, rutile TiO<sub>2</sub> is known to function well as a photocatalyst during the oxidation of water into molecular O<sub>2</sub> under band gap irradiation.<sup>4</sup> Even in the presence of electron donors such as Fe<sup>2+</sup> or I<sup>−</sup> that can hinder water oxidation, this compound is capable of selectively oxidizing water.<sup>5,6</sup> Based on this property, rutile TiO<sub>2</sub> is able to function as a vital component of O<sub>2</sub> evolution in a Z-scheme water-splitting system in combination with a suitable H<sub>2</sub> evolution photocatalyst and a shuttle redox mediator.<sup>6–8</sup> It has also been demonstrated that rutile TiO<sub>2</sub> works more efficiently than PtO<sub>x</sub>/WO<sub>3</sub>, a well-known visible-light-responsive photocatalyst, when employed in a Z-scheme water-splitting system operating under simulated sunlight and coupled with Pt/BaZrO<sub>3</sub>–BaTaO<sub>2</sub>N, a narrow band gap semiconductor that works as the H<sub>2</sub> evolution component.<sup>8</sup> Very recently, rutile TiO<sub>2</sub> has

been explored as a new photocatalyst capable of splitting pure water into H<sub>2</sub> and O<sub>2</sub> under band gap irradiation.<sup>9</sup>

In general, the functionality (such as the photocatalytic activity) of a given material is strongly dependent on the physicochemical properties of that substance.<sup>2b,d</sup> Therefore, investigating the relationship between the functionality and physicochemical characteristics of a material is of interest, because it can be expected to provide useful information to allow further refinement of such systems. Previous studies have suggested that the water oxidation activity of rutile TiO<sub>2</sub> is increased with an increase in its secondary particle size.<sup>10</sup> Matsumura et al. claimed that band-bending is needed for water oxidation involving a 4-electron process, and that such band-bending is readily generated in larger particles.<sup>11</sup> The reaction mechanism of water oxidation occurring on the surface of rutile TiO<sub>2</sub> has been studied by Nakamura et al.<sup>12</sup> To date, however, the relationship between the photocatalytic water oxidation activity (especially in the presence of a reversible electron acceptor) and physicochemical properties of rutile TiO<sub>2</sub> has yet to be determined, and the factor(s) affecting the activity remain unknown.

In this study, rutile TiO<sub>2</sub> particles with sizes ranging from several tens of nanometers to a few micrometers were prepared by simply heating rutile TiO<sub>2</sub> nanopowder in air at different temperatures. These materials were then examined as photo-

Received: February 6, 2014

Revised: April 5, 2014

Published: April 21, 2014

catalysts for water oxidation in the presence of a reversible electron acceptor ( $\text{IO}_3^-$  or  $\text{Fe}^{3+}$ ). Factors affecting the activity are discussed on the basis of the results of physicochemical analyses and photocatalytic reactions.

A nanoparticulate rutile  $\text{TiO}_2$  sample (JRC-TiO-6) was supplied by the Catalysis Society of Japan and was subject to heating at 873–1273 K for 2 h in air. The calcined samples are hereafter referred to as R- $T$ , where  $T$  indicates the calcination temperature.

The as-prepared rutile  $\text{TiO}_2$  samples were studied by X-ray diffraction (XRD; MiniFlex 600, Rigaku), UV–visible diffuse reflectance spectroscopy (DRS; V-565, Jasco), and scanning electron microscopy (SEM; S-4700, Hitachi). The Brunauer–Emmett–Teller (BET) surface areas of these samples were also measured, using a BELSORP-mini (BEL Japan) at liquid nitrogen temperature (77 K).

Reactions were conducted in a Pyrex top-irradiation vessel connected to a glass closed gas circulation system. In such trials, a 100 mg sample of rutile  $\text{TiO}_2$  powder was dispersed in an aqueous solution (100 mL) of either 10 mM  $\text{NaIO}_3$  (Kanto Chemicals) or 10 mM  $\text{FeCl}_3 \cdot 4\text{H}_2\text{O}$  (Kanto Chemicals) using a magnetic stirrer. The reactant solution was evacuated several times to completely remove air, and a small amount of Ar gas (approximately 5 kPa) was introduced into the reaction system prior to irradiation under a 300 W xenon lamp (Cermac, PE300BF) with an output current of 20 A. The irradiation wavelength was controlled by a cold mirror and water filter ( $\lambda > 350$  nm). The reactant solution was maintained at room temperature by a water bath during the reaction and the evolved gases were analyzed by gas chromatography (Shimadzu, GC-8A with TCD detector and MS-5A column, argon carrier gas). When analyzing only oxygen, helium is much better as a carrier gas than argon. However, due to the requirement to examine possible production of hydrogen via water reduction, argon was used to quantify both hydrogen and oxygen.

Figure 1 shows the XRD patterns of the prepared samples. All of the prepared samples exhibit single-phase diffraction

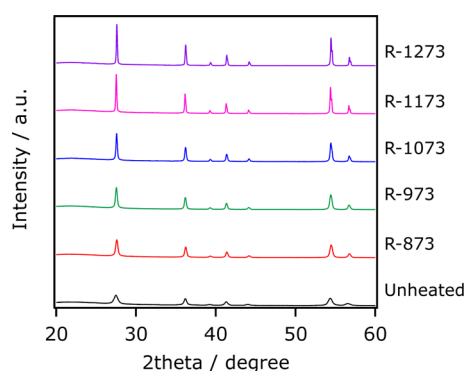


**Figure 1.** XRD patterns of the prepared rutile  $\text{TiO}_2$  samples.

patterns assigned to rutile  $\text{TiO}_2$  without any evidence of an impurity phase. The diffraction peaks of the rutile  $\text{TiO}_2$  become more intense and narrower as the calcination temperature increases, indicative of improved crystallinity at higher temperatures. This behavior is also supported by the results of SEM observations. As shown in Figure 2, the particles of untreated rutile  $\text{TiO}_2$  were irregularly shaped with sizes on the order of several tens of nanometers, whereas the materials calcined at elevated temperatures became more regular and

enlarged with increasing the calcination temperature. Specific surface areas of these samples as determined by nitrogen adsorption at 77 K are presented in Table 1, and the observed trend in these data is in good agreement with that seen in the SEM images (Figure 2). UV–visible diffuse reflectance spectroscopy (Figure S1) showed that all of the prepared samples had an absorption edge at ca. 410 nm (corresponding to a 3.0 eV band gap), although there was a small difference in absorption profiles among the samples.

Water oxidation reactions were performed using the as-prepared rutile  $\text{TiO}_2$  samples. Table 1 summarizes the photocatalytic activities of rutile  $\text{TiO}_2$  specimens calcined at different temperatures for water oxidation in aqueous solutions containing  $\text{NaIO}_3$  or  $\text{FeCl}_3$ . All the tested samples were found to produce  $\text{O}_2$  upon UV irradiation, although the specific activities obtained were highly dependent on the calcination temperature. Previous studies have indicated that the conversion of  $\text{IO}_3^-$  and  $\text{Fe}^{3+}$  over rutile  $\text{TiO}_2$  photocatalyst was very efficient.<sup>5,6</sup> In this study, stoichiometric conversion of reactants ( $\text{IO}_3^-$  and  $\text{Fe}^{3+}$ ) was actually confirmed with no  $\text{H}_2$  evolution (see  $\text{Fe}^{3+}$  case for example, Figure S2). The measured rates of  $\text{O}_2$  evolution can be seen to increase with increasing calcination temperature, eventually reaching a maximum at 1073 K after which the rates begin to drop. This trend, in which rates increase and then fall, was observed when using both  $\text{NaIO}_3$  and  $\text{FeCl}_3$ , suggesting that the change in activity is independent of the particular electron acceptor employed. However, the performance of a give rutile sample was different with respect to the electron acceptor employed. It should be first noted that the reaction pH value is different from each other in these two reactions: pH  $\sim 6$  in the  $\text{NaIO}_3$  system, and pH  $\sim 2.5$  in the  $\text{FeCl}_3$  system. As photocatalytic reaction rate is in general dependent on the pH of the reactant solution,<sup>2d</sup> the difference could cause the activity difference between the two system. Another plausible explanation is that the reduction of  $\text{IO}_3^-$  ions involves six electrons, while that of  $\text{Fe}^{3+}$  just one electron. Thus, the former is kinetically more difficult to proceed than the latter. This could explain why the  $\text{Fe}^{3+}$  system gave a higher rate of  $\text{O}_2$  evolution than the  $\text{IO}_3^-$  system. However, this is not the case for the unheated sample. Thus, there would be some unknown factor(s) that can affect the activity, which will be examined in the next work.

The enhancement of activity with increasing calcination temperature up to 1073 K is most likely due to crystallization of the rutile particles, as can be seen from the results of XRD and SEM analyses (Figures 1 and 2). Crystallization of semiconductor particles increases the lifetime of photogenerated charge carriers prior to recombination, resulting in enhanced photocatalytic activity.<sup>2b,d</sup> Although a larger specific surface area is favorable, because it leads to increased adsorption of reactants, it appears that improved crystallinity and the concomitant long-lived electron–hole pairs are more important with regard to the enhancement of the water oxidation reaction by rutile  $\text{TiO}_2$ . This trend is consistent with previous reports that larger rutile  $\text{TiO}_2$  particles tend to exhibit higher photocatalytic water oxidation activity, and therefore, it is reasonable to expect that the water oxidation activity would be steadily increased with the application of higher calcination temperatures, because high temperature calcination causes the growth of rutile particles. The data in Table 1, however, show that this was not the case.

Li et al. have reported that the treatment of rutile  $\text{TiO}_2$  nanowire arrays with  $\text{H}_2$  at 623–773 K increased the density of

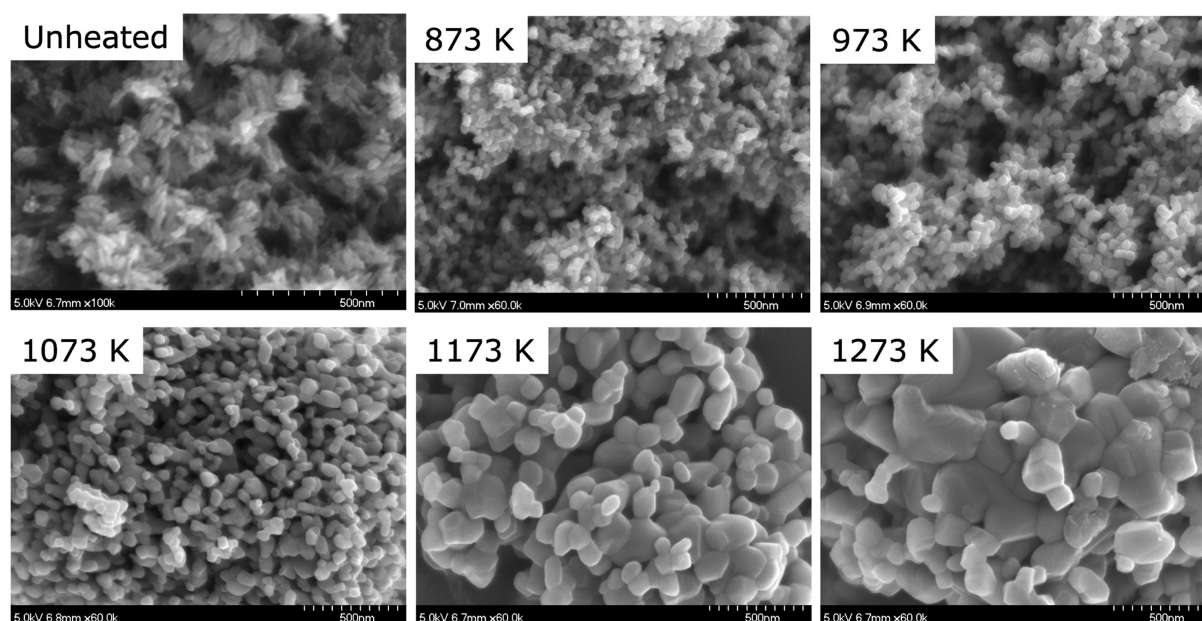


Figure 2. SEM images of the prepared rutile  $\text{TiO}_2$  samples.

Table 1. Specific Surface Areas and Photocatalytic Activities of Rutile  $\text{TiO}_2$  Samples Calcined at Different Temperatures during Water Oxidation in the Presence of  $\text{IO}_3^-$  or  $\text{Fe}^{3+}$  as an Electron Acceptor under UV Irradiation ( $\lambda > 350 \text{ nm}$ )<sup>a</sup>

| entry | calcination temperature (K) | specific surface area ( $\text{m}^2 \text{g}^{-1}$ ) | $\text{O}_2$ evolution rate <sup>b</sup> ( $\mu\text{mol h}^{-1}$ ) |                               |
|-------|-----------------------------|--|---|-------------------------------|
|       |                             |  | from $\text{NaIO}_3$ solution                                       | from $\text{FeCl}_3$ solution |
| 1     |                             | 85   | 10.0  | <0.5                          |
| 2     | 873                         | 34   | 17.8  | 27.6                          |
| 3     | 973                         | 29   | 25.2  | 34.8                          |
| 4     | 1073                        | 17   | 28.2  | 44.1                          |
| 5     | 1173                        | 5.8  | 11.8  | 38.2                          |
| 6     | 1273                        | 2.3  | 3.3   | 22.7                          |

<sup>a</sup>Reaction conditions: catalyst, 100 mg; reactant solution, 100 mL (10 mM), xenon lamp (300 W) fitted with a cold mirror (CM-1).

<sup>b</sup>Average rate in 2 h.

oxygen vacancies, leading to an increase in donor density.<sup>13</sup> This improved donor density results in prompt charge

transport, and so the treated rutile  $\text{TiO}_2$  electrode exhibited enhanced performance during photoelectrochemical water oxidation compared to an untreated control electrode. Based on this result, heat treatment of rutile  $\text{TiO}_2$  under an oxygen-containing atmosphere such as static air should reduce the density of oxygen vacancies. Consequently, it is considered that the high temperature calcination of rutile  $\text{TiO}_2$  in air reduces the density of oxygen vacancies, which is disadvantageous in terms of prompt migration of photogenerated charge carriers in the semiconductor solid, thereby lowering the material's activity.  $\text{TiO}_2$  is a typical nonstoichiometric compound and can be best expressed by the oxygen-deficient formula  $\text{TiO}_{2-x}$ .<sup>14</sup> The stoichiometry is to some extent controllable by changing temperature and oxygen activity. For example, high temperature calcination in air reduces the number of oxygen vacancies in  $\text{TiO}_2$ ,<sup>14,15</sup> although under extremely strong oxidative conditions, the generation of Ti defects occurs, resulting in p-type semiconductivity.<sup>14</sup>

To confirm the validity of this theory, R-1073 was subject to heating under a flow of  $\text{H}_2$  (20  $\text{mL min}^{-1}$ ) at 673 K for 1 h to

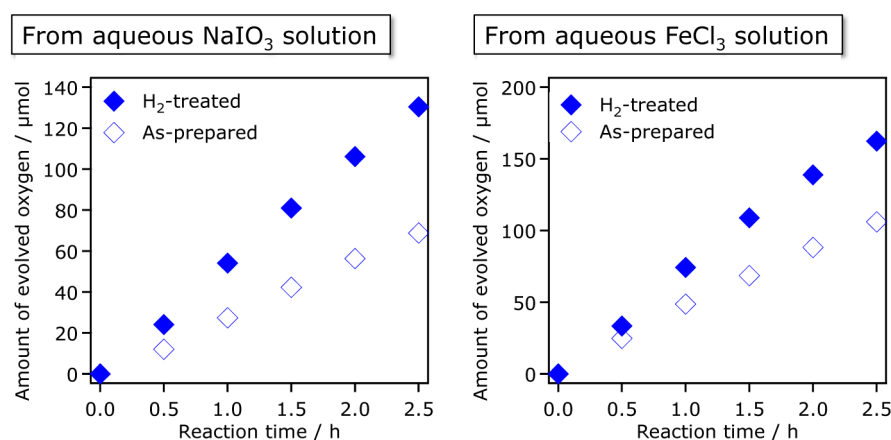
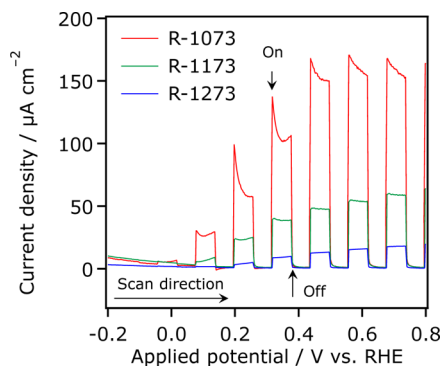


Figure 3. Time courses of  $\text{O}_2$  evolution from R-1073 in aqueous  $\text{NaIO}_3$  and  $\text{FeCl}_3$  solutions under UV irradiation. Reaction conditions: catalyst, 100 mg; reactant solution, 100 mL (10 mM), xenon lamp (300 W) fitted with a cold mirror (CM-1).

increase the density of oxygen vacancies. XRD and SEM analyses showed that no structural changes had occurred during this treatment, as shown in Figure S3, although an additional absorption feature was observed at longer wavelengths in the diffuse reflectance spectrum, possibly resulting from the introduction of oxygen vacancies and the concomitant formation of  $\text{Ti}^{3+}$ .<sup>15</sup> A further indication of the increased density of oxygen vacancies was the color change of the samples after  $\text{H}_2$ -reduction treatment; the R-1073 following calcination in air was white while the material was a light gray after  $\text{H}_2$ -treatment.

As expected, the  $\text{O}_2$  evolution activity of the R-1073 was improved following the  $\text{H}_2$ -treatment (Figure 3), regardless of the electron acceptor employed. The activity of the  $\text{H}_2$ -treated sample was almost the same as that achieved using one of the most active rutile  $\text{TiO}_2$  (HT0210),<sup>16</sup> which has been reported by Abe et al.<sup>6b</sup> It is noteworthy that R-1073, which exhibited the highest activity among the samples prepared, was further enhanced by this treatment, because this indicates that there are at least two mutually opposing factors affecting the activity of the material. These factors, high crystallinity and high oxygen vacancy density, are improved and degraded by high temperature calcination, respectively. Additional tests also demonstrated that  $\text{H}_2$ -reduction treatment was an effective means of improving the R-1273, which had been subject to heating in air at the highest temperature and had exhibited relatively low activity. As shown in Figure S5, however, the enhancement of the R-1273 activity was moderate compared to the improvement observed in the case of the R-1073. Presumably the present treatment condition may not be sufficiently optimized to regenerate the donor concentration in R-1273, because the density of oxygen vacancies in R-1273 is predicted to be lower than that in R-1073. Thus, it is reasonable to conclude that photocatalytic activity for water oxidation by rutile  $\text{TiO}_2$  is dependent on both the crystallinity and the density of oxygen vacancies. Amano et al. have very recently reported a similar enhancement of the activity of rutile  $\text{TiO}_2$  powder for  $\text{H}_2$  evolution from a water–methanol mixture by  $\text{H}_2$ -reduction treatment.<sup>15</sup>

Further evidence of the negative impact of high-temperature calcination on water oxidation activity was provided by photoelectrochemical analysis.<sup>17,18</sup> As shown in Figure 4, the anodic photocurrents generated from porous rutile  $\text{TiO}_2$  electrodes were decreased with increasing calcination temperature over the entire potential range examined. This is due to a



**Figure 4.** Current–voltage curves obtained from aqueous 0.1 M  $\text{Na}_2\text{SO}_4$  solution (pH = 5.9) under intermittent UV irradiation ( $\lambda > 350$  nm) using rutile  $\text{TiO}_2$  electrodes ( $5.25$   $\text{cm}^2$ ). Scan rate:  $20$   $\text{mV s}^{-1}$ .

decrease in the density of oxygen vacancies (in other words, the donor density or n-type semiconducting character) in the rutile  $\text{TiO}_2$  particles resulting from the application of elevated temperatures.<sup>13</sup> It is also noteworthy that the degree of the decrease in performance with respect to calcination temperature is more pronounced in the lower potential region, indicating that water oxidation on the surface of rutile  $\text{TiO}_2$  becomes less favored kinetically as the calcination temperature is increased. Another noticeable observation in the current–voltage curves is that the anodic photocurrent generated from the R-1073 electrode underwent saturation at applied potentials of  $0.4$ – $0.8$  V vs RHE, probably due to the surface reaction being the rate-determining step, independent of the applied potential and/or the existence of relatively large resistance in the electrode structure, as has been observed in some photoelectrode systems.<sup>2c,19</sup>

Although rutile  $\text{TiO}_2$  works better as an  $\text{O}_2$  evolution photocatalyst than  $\text{WO}_3$  in some Z-scheme systems as mentioned in the introduction,<sup>8</sup> it may seem that the performance of the present rutile electrodes for photoelectrochemical water oxidation is not very high, compared to that of  $\text{WO}_3$  photoanodes recorded under similar conditions.<sup>20</sup> However, it is impossible to just simply compare the performance of the present rutile electrodes with that of  $\text{WO}_3$ , because (1) photocatalytic reaction systems are different from photoelectrode systems in terms of energy input, and (2) the efficiency of the electrode material depends strongly on the various parameters such as feature size, carrier concentration, resistance in the electrode structure, and so on.<sup>2c</sup> A plausible explanation of the relatively low current density of the present electrode samples is that the optimization has not been done in terms of the particle size of rutile and the preparation conditions of electrode.

In summary, water oxidation to generate  $\text{O}_2$  was examined using rutile  $\text{TiO}_2$  particles in the presence of either  $\text{IO}_3^-$  or  $\text{Fe}^{3+}$  as a reversible electron acceptor. It was found that the photocatalytic activity of the  $\text{TiO}_2$  depends on both the crystallinity and the density of oxygen vacancies, both of which are determined by the preparation conditions. Calcination of nanoparticulate rutile  $\text{TiO}_2$  in air resulted in crystallization, leading to enhanced activity for the oxidation reaction. High-temperature calcination in air, however, also reduced the density of oxygen vacancies and degraded the material's charge transport properties, which in turn lowered the activity. Additional post-treatment of the rutile  $\text{TiO}_2$  with  $\text{H}_2$  gas was effective at improving its activity, because this treatment increased the density of oxygen vacancies. This simple technique involving enhancement via  $\text{H}_2$  reduction may be applicable to other metal oxide semiconductor particles that are active for photocatalytic water oxidation, and this possibility is currently being investigated. It is also important to directly measure the lifetime of electrons and holes in rutile  $\text{TiO}_2$  samples by means of physicochemical methods including time-resolved spectroscopy.<sup>15,21</sup> As such measurements would give us useful information, they will be done as part of future works.

## ■ ASSOCIATED CONTENT

### Supporting Information

XRD patterns, UV–visible diffuse reflectance spectra, SEM images, and photocatalytic reaction data. This material is available free of charge via the Internet at <http://pubs.acs.org>.

## ■ AUTHOR INFORMATION

## Corresponding Author

\*E-mail: maedak@chem.titech.ac.jp. Fax: +81-3-5734-2284. Tel.: +81-3-5734-2239.

## Notes

The authors declare no competing financial interest.

## ■ ACKNOWLEDGMENTS

This work was supported by the PRESTO/JST program "Chemical Conversion of Light Energy" and a Grant-in-Aid for Young Scientists (A) (project no. 25709078) as well as a support program for people raising children by the Gender Equality Center (GEC) at the Tokyo Institute of Technology. The author would like to thank Profs. Takashi Hisatomi and Kazunari Domen (University of Tokyo) for assistance in SEM observations. The author also acknowledges the Catalysis Society of Japan and Toho Titanium Co. for kindly supplying their TiO<sub>2</sub> samples (JRC-TIO-6 and HT0210, respectively).

## ■ REFERENCES

- (1) Fujishima, A.; Honda, K. *Nature* **1972**, *238*, 37–38.
- (2) (a) Bard, A. J.; Fox, M. A. *Acc. Chem. Res.* **1995**, *28*, 141–145. (b) Kudo, A.; Miseki, Y. *Chem. Soc. Rev.* **2009**, *38*, 253–278. (c) Abe, R. *J. Photochem. Photobiol. C* **2010**, *11*, 179–209. (d) Maeda, K. *J. Photochem. Photobiol. C* **2011**, *12*, 237–268. (e) Maeda, K. *ACS Catal.* **2013**, *3*, 1486–1503.
- (3) Fujishima, A.; Rao, T. N.; Tryk, D. A. *J. Photochem. Photobiol. C* **2000**, *1*, 1–21.
- (4) (a) Nishimoto, S.; Ohtani, B.; Kajiwara, H.; Kagiya, T. *J. Chem. Soc., Faraday Trans. 1* **1985**, *81*, 61–68. (b) Oosawa, Y.; Grätzel, M. *J. Chem. Soc., Faraday Trans. 1* **1988**, *84*, 197–205.
- (5) Ohno, T.; Haga, D.; Fujihara, K.; Kaizaki, K.; Matsumura, M. *J. Phys. Chem. B* **1997**, *101*, 6415–6419.
- (6) (a) Abe, R.; Sayama, K.; Domen, K.; Arakawa, H. *Chem. Phys. Lett.* **2001**, *344*, 339–344. (b) Abe, R.; Sayama, K.; Sugihara, H. *J. Phys. Chem. B* **2005**, *109*, 16052–16061.
- (7) Kato, H.; Hori, M.; Kōta, R.; Shimodaira, Y.; Kudo, A. *Chem. Lett.* **2004**, *33*, 1348–1349.
- (8) Maeda, K.; Lu, D.; Domen, K. *ACS Catal.* **2013**, *3*, 1026–1033.
- (9) Maeda, K. *Chem. Commun.* **2013**, *49*, 8404–8406.
- (10) (a) Ikeda, S.; Sugiyama, N.; Murakami, S.; Kominami, H.; Kera, Y.; Noguchi, H.; Uosaki, K.; Torimoto, T.; Ohtani, B. *Phys. Chem. Chem. Phys.* **2003**, *5*, 778–783. (b) Prieto-Mahaney, O.-O.; Murakami, N.; Abe, R.; Ohtani, B. *Chem. Lett.* **2009**, *38*, 238–239.
- (11) Ohno, T.; Sarukawa, K.; Matsumura, M. *New J. Chem.* **2002**, *22*, 1167–1170.
- (12) (a) Nakamura, R.; Nakato, Y. *J. Am. Chem. Soc.* **2004**, *126*, 1290–1298. (b) Nakamura, R.; Okamura, T.; Ohashi, N.; Imanishi, A.; Nakato, Y. *J. Am. Chem. Soc.* **2005**, *127*, 12975–12983.
- (13) Wang, G.; Wang, H.; Ling, Y.; Tang, Y.; Yang, X.; Fitzmorris, R. C.; Wang, C.; Zhang, J. Z.; Li, Y. *Nano Lett.* **2011**, *11*, 3026–3033.
- (14) Nowotny, M. K.; Sheppard, L. R.; Bak, T.; Nowotny, J. *J. Phys. Chem. C* **2008**, *112*, 5275–5300.
- (15) Amano, F.; Nakata, M.; Asami, K.; Yamakata, A. *Chem. Phys. Lett.* **2013**, *579*, 111–113.
- (16) The HT0210 sample, which was supplied from Toho Titanium Co, contained rutile as the main phase with a tiny portion of anatase. It has been reported to show activity for water oxidation in the presence of IO<sub>3</sub><sup>-</sup> ions under UV irradiation, exhibiting an apparent quantum yield of ca. 10% at 350 nm at the optimal condition (ref 6b). Under the present reaction condition, the sample produced O<sub>2</sub>, which was almost the same level as that achieved using the H<sub>2</sub>-reduced R-1073 (Figure S4).
- (17) Porous electrodes of rutile TiO<sub>2</sub> were prepared by pasting viscous slurry onto conducting glass according to a conventional squeeze method. A mixture of 50 mg of rutile TiO<sub>2</sub> powder, 10 μL of acetylacetone (Kanto Chemicals), 10 μL of TritonX (Aldrich, U.S.A.), 10 μL of poly(ethylene glycol) 300 (Kanto Chemicals), and 500 μL of distilled water was ground in an agate mortar to prepare the viscous slurry. The slurry was then pasted onto fluorine-doped tin-oxide (FTO) glass slides (thickness 1.8 mm; Asahi Glass, Japan) to prepare a 1.5 × 3.5 cm<sup>2</sup> electrode, and the sample was calcined in air at 723 K for 1 h.
- (18) Photoelectrochemical measurements were carried out with a potentiostat (HSV-110, Hokuto Denko) and an electrochemical cell at room temperature. The cell was made of Pyrex glass, and was a three-electrode-type system using Pt wire and an Ag/AgCl electrode as the counter and reference electrodes, respectively. A Na<sub>2</sub>SO<sub>4</sub> aqueous solution (pH = 5.9) was used as the electrolyte, which was saturated with argon gas prior to the electrochemical measurements. The light source was a xenon lamp (300 W) fitted with a cold mirror (λ > 350 nm). The potential of the photoelectrode is reported against the reversible hydrogen electrode (RHE):  $E_{\text{RHE}} = E_{\text{AgCl}} + 0.059 \text{ pH} + E_{\text{AgCl}}^{\circ}$  ( $E_{\text{AgCl}}^{\circ} = 0.1976 \text{ V at } 298 \text{ K}$ ).
- (19) Sivula, K.; Le Formal, F.; Grätzel, M. *ChemSusChem* **2011**, *4*, 432–449.
- (20) Ma, S. S. K.; Maeda, K.; Abe, R.; Domen, K. *Energy Environ. Sci.* **2012**, *5*, 8390–8397.
- (21) Carneiro, J. T.; Savenije, T. J.; Moulijn, J. A.; Mul, G. *J. Phys. Chem. C* **2010**, *114*, 327–332.